

Heterogeneous robots coordination for industrial plant inspection and evaluation at World Robot Summit 2020

Shotaro Kojima, Tomoya Takahashi, Ranulfo Bezerra, Takaaki Nara, Masaki Takahashi, Naoto Saiki, Kenta Gunji, Pongsakorn Songsuroj, Ryota Suzuki, Kotaro Sato, Zitong Han, Kagetora Takahashi, Yoshito Okada, Masahiro Watanabe, Kenjiro Tadakuma, Kazunori Ohno & Satoshi Tadokoro

To cite this article: Shotaro Kojima, Tomoya Takahashi, Ranulfo Bezerra, Takaaki Nara, Masaki Takahashi, Naoto Saiki, Kenta Gunji, Pongsakorn Songsuroj, Ryota Suzuki, Kotaro Sato, Zitong Han, Kagetora Takahashi, Yoshito Okada, Masahiro Watanabe, Kenjiro Tadakuma, Kazunori Ohno & Satoshi Tadokoro (2022) Heterogeneous robots coordination for industrial plant inspection and evaluation at World Robot Summit 2020, Advanced Robotics, 36:21, 1102-1119, DOI: [10.1080/01691864.2022.2111230](https://doi.org/10.1080/01691864.2022.2111230)

To link to this article: <https://doi.org/10.1080/01691864.2022.2111230>



© 2022 The Author(s). Published by Informa UK Limited, trading as Taylor & Francis Group and The Robotics Society of Japan.



Published online: 26 Aug 2022.



Submit your article to this journal 



Article views: 920



View related articles 



View Crossmark data 



Citing articles: 3 View citing articles 



Heterogeneous robots coordination for industrial plant inspection and evaluation at World Robot Summit 2020

Shotaro Kojima^{a,b}, Tomoya Takahashi^c, Ranulfo Bezerra^b, Takaaki Nara^c, Masaki Takahashi^c, Naoto Saiki^c, Kenta Gunji^c, Pongsakorn Songsuroj^c, Ryota Suzuki^c, Kotaro Sato^c, Zitong Han^c, Kagetora Takahashi^c, Yoshito Okada^b, Masahiro Watanabe^b, Kenjiro Tadakuma^{b,c}, Kazunori Ohno^{b,a,b} and Satoshi Tadokoro^{b,c}

^aNew Industry Creation Hatchery Center (NICHe), Tohoku University, Sendai, Japan; ^bTough Cyberphysical AI Research Center (TCPAl), Tohoku University, Sendai, Japan; ^cGraduate School of Information Sciences, Tohoku University, Sendai, Japan

ABSTRACT

This paper describes a plant inspection robot team consisting of three types of robots that won the World Robot Summit 2020 plant disaster prevention challenge. There is a social demand to use robots for industrial plant inspection tasks to decrease the workload and risks of human operators. In this study, the authors developed a plant inspection system using a tracked vehicle, a mecanum-wheeled vehicle, and an unmanned aerial vehicle (UAV). The roles between work-related tasks and visual inspection tasks are divided by two operators, resulting in efficient operation. Experimental results show that the tracked vehicle can conduct challenging tasks such as climbing up the stairs and large-valve operations. The results also showed that the visual inspection task was performed 58% faster by the mecanum vehicle in a narrow passage and 48% faster by the UAV on the stairs, as compared with the tracked vehicle in the same situations. The analysis of the competition results showed that we obtained points in 57% (160/280) of the work-related tasks and 85% (170/200) of the visual inspection tasks as well as 92% (110/120) of the emergency response tasks in the final round.

ARTICLE HISTORY

Received 1 March 2022

Revised 14 June 2022

Accepted 12 July 2022

KEYWORDS

Industrial plant inspection;
disaster response; World
Robot Summit

1. Introduction

Recently, the introduction of robots for industrial plant inspections has been promoted on a global scale in order to reduce the workload and risks to human operators. Sprint Robotics, which is a collaborative organization of industry-led initiatives, formulated a roadmap for automating industrial plant inspection using robots [1]. The roadmap shows the target environments, required abilities of robots, and current achievable level. This book is a reference for the introduction of inspection robots into existing industrial facilities.

To promote the development of industrial plant inspection robot systems, the World Robot Summit (WRS) plant disaster prevention challenge [2] was held. This competition was designed to provide a place for promotion and acceleration of research and development and demonstration experiments, considering the former successful competitions such as DARPA Challenge [3, 4], AUVSI International Aerial Robotics Competition [5], and RoboCup [6]. These competitions have played important roles in accelerating the robot development and promoting the use of robotics technologies in the real world. The WRS plant disaster prevention challenge was

designed to evaluate the performance of the robotic systems according to [1], from which the following actions were drawn:

- traversing inspection passage, including flat floor, narrow passage, steep staircases, and cage ladders;
- operating large and heavy valves;
- monitoring atmosphere (smell and gas leak);
- reading dial (analog gauge);
- emergency response.

In this competition, the tasks above were conducted by robots in a limited time, and points were assigned for each task. The maximum number of remote human operators was two, considering the limitation of human resources in real situations. Meanwhile, the number of robots was not limited as long as they fitted in a 1.2 m square starting area. The authors assume that this regulation reflects the mention on the use of multiple robots in [1], which says ‘Multiple robots may be needed to fulfil any of the above-described roles’.

The authors won the WRS 2020 plant disaster prevention challenge with a robot system consisting of three

types of robots: a tracked vehicle with six degrees-of-freedom (DoF) manipulator, a mecanum-wheeled vehicle, and an unmanned aerial vehicle (UAV). Table 1 shows the features and task coverage of each robot. The tracked vehicle ‘Onix’ was designed to cover all the tasks except for the accessibility to cage ladders. In addition, the mecanum-wheeled vehicle and the UAV were used for increasing the time-efficiency of the visual inspection such as analog gauge reading. Mecanum-wheeled vehicle is suitable for tasks in narrow spaces because of its high positioning accuracy and smaller footprint, as compared with the tracked vehicle. The UAV has high accessibility to high positions, which cannot be achieved or take time for ground vehicles. The authors divided the roles into two operators: one was in charge of a work-related tasks using the tracked vehicle Onix, and another was in charge of visual inspection using the mecanum-wheeled vehicle and the UAV.

In the plant inspection scenario using robots, the individual and total performance of different types of robots should be verified. The authors aim to increase the time efficiency by separating roles by robots as mentioned above, where individual and total performance tests are required. These tests show the effectiveness of the use of different robots and how the current system can be improved considering the total performance in the competition.

This paper describes the details of the plant inspection system using three different types of robots and its performance tests. The individual test results show that the visual inspection task is performed 58% faster when the mecanum vehicle is used in a narrow passage and 48% faster when the UAV is used on the stairs, as compared with the tracked vehicle in the same situations. The analysis of the competition results shows that we obtained points in 57% (160/280) of the work-related tasks and 85% (170/200) of the visual inspection tasks as well as 92% (110/120) of the emergency response tasks in the final round. Such a performance is achieved by the visual inspection speed of the UAV and mecanum vehicle and the design of the tracked vehicle that can handle challenging tasks such as large valve operation.

The main contribution of this paper is as follows:

- The authors developed a tracked vehicle Onix that can complete plant inspection tasks, including challenging tasks such as operating large and heavy valves.
- Individual tests of the tasks were conducted for each robot in the laboratory, and the suitability of each robot was clarified.
- The competition results were analyzed as the total performance. The results revealed the following advantages of our system: fast visual inspection by the

mecanum-wheeled vehicle and the UAV and good performance of work-related tasks (high score) operated by the tracked vehicle. In addition, the results revealed the room of improvement such as effective use of time after the visual inspection was completed.

2. Related work

The industrial plant inspection system is being actively developed, and several companies have developed robot systems for commercial use. Mitsubishi Heavy Industry developed a tracked vehicle for a petroleum refining plant [7]. They also developed nuclear power plant inspection robot MEISTeR [8], used in the Fukushima Daiichi nuclear power plant for the sample-return mission. Furthermore, Taurob develops plant inspection robot systems [9] and searches for new markets of robot systems, for example, fire department, mining industry, and nuclear industry in addition to the petroleum industry. The similarities of these robot systems are use of a tracked vehicle with a manipulator as a platform and high environmental resistance such as being explosion-, water-, or dust-proof. Moreover, several functions described in ‘innovation landscape map remote operator’ shown in [1] have already been realized, for example, remote manual or fully autonomous monitoring operation on a flat surface and emergency response with manual operation. Meanwhile, [1] also mentions that there are ‘capability gaps,’ such as accessing cage-ladders, operating valves, including heavy ones, or advanced and full autonomy. The authors tackle these challenges through the competition. In particular, our system solves one of the capability gaps: heavy-valve operation.

Several research groups reported the results of competitions of plant inspection robots, including their strategy, system design, results, or lessons learned. After the pre-tournament of the WRS plant disaster prevention challenge held in 2018, team AiSafe [10] and UEC snake with Tohoku Gripper [11, 12] reported their performance. In [10], an inspection system was constructed with a tracked vehicle and a UAV. They were ranked third place in the competition, and they reported the advantage of combining a ground vehicle with an aerial vehicle. In [11, 12], a snake-like robot was used as a platform, and stair climbing as well as valve operation, being challenging tasks for snake-like robots, were realized. The authors constructed a system with a tracked vehicle, UAV, and mecanum-wheeled vehicle. The combination of aerial and ground vehicles is common in [10]. In addition, the authors attempted to increase the accessibility to narrow passages using a mecanum vehicle with reference to [11], wherein high accessibility of a snake-like robot in narrow

Table 1. Features and task coverage of each robot of the proposed system.

	Onix	Mecanum rover	UAV (DJI Mavic 2)
			
Chassis	Tracked vehicle with six DoF arm	Mecanum wheeled vehicle	Quadrotor
Size (mm)	L760 × W600 × H450	L398 × W349 × H1200	L497 × W431 × H82
Weight (kg)	40	20	0.9
Operating time (h)	3.0	6.0	0.5
Sensors	Visual camera × 5 3D LIDAR × 1 Thermal camera × 1 CO2 sensor × 1	Visual camera × 5 3D LIDAR × 2	Visual camera × 1 Vision sensor × 4 (for collision avoidance)
Gauge recognition	✓	✓	✓
3D mapping	✓	✓	✗
Valve operation	✓	✗	✗
Narrow space access	✓	✓	✓
Stair access	✓	✗	✓
Ladder access	✗	✗	✓

Notes: Tracked vehicle 'Onix' was designed to cover all tasks and terrains, except accessibility to ladders. To increase the time efficiency, mecanum rover and UAV were introduced for the visual inspection in narrow space and in high positions, respectively.

passages was achieved. This situation is difficult for a tracked vehicle or a UAV.

3. Plant inspection system with three different-type robots

3.1. Outline

The target tasks and environments have been described previously [2, 13]. The field consists of a flat floor, narrow passage, catwalk including stairs, and grating areas. Simulated facilities such as a boiler, water tanks, pipes with gauges and valves, and motor pumps are located in the field. In this environment, the robots should deal with the following tasks:

- analog gauge reading (autonomous recognition);
- water level reading (autonomous recognition);
- LED control panel reading;
- abnormal heat detection on pipe surface;
- valve operation (lever or circular);
- gas leak detection (CO2).

Especially, the number of analog gauges and valves is particularly large (30 and 32 installed in the environment, respectively). Moreover, these tasks are used not only in preliminary rounds but also in the finals. Thus, the authors focused on how to efficiently deal with these tasks in a limited time by two operators.

Our basic strategy was to divide the roles by valve operation and visual inspection with two operators and use different types of robots considering the aptitude of each robot. The first operator operates the tracked

vehicle Onix, which deals with valves and other tasks such as heat detection or gas leak detection, because these tasks require the manipulator to operate the target or to adjust sensor's position. Onix has high mobility; therefore, it covers all the above-mentioned terrains. The second operator operates the mecanum rover and the UAV, which deal with visual inspection (analog gauge reading, LED control panel reading) using cameras. The UAV covers open space, including catwalk, because it can quickly access the target in such situations. The mecanum rover was used in narrow passages considering its high positioning accuracy and small footprint because UAVs tend to be slow in narrow passages to avoid collisions. The authors gave up some tasks, such as an autonomous reading of water level or large valve operation in the highest positions, because they take a significantly long time compared to the expected score or required development in different approaches.

Figure 1 shows the entire system configuration. In this system, robots are remotely operated from the operator's booth via wireless communication. A tracked vehicle, mecanum-wheeled vehicle, and UAV are used as robot platform that covers the tasks as shown in Table 1. Laptop computers are located in the operator's booth for each robot and used for controlling and monitoring robots or executing autonomous recognition of the visual inspection target. The tracked and mecanum-wheeled vehicles are operated using a laptop computer in the operator's desk via Wi-Fi communication. The UAV is controlled using a remote controller that shows a camera stream. The camera image is transmitted to a laptop computer to execute the recognition. Autonomous recognition software is used for each robot.

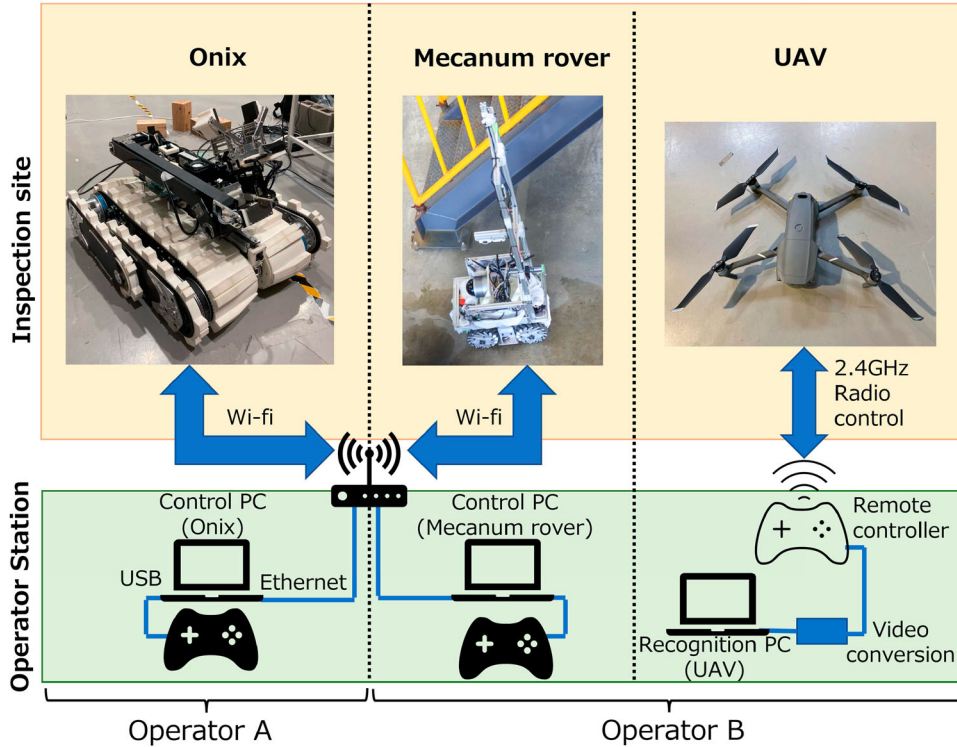


Figure 1. Entire system configuration of three different-type robots. Robots are remotely operated via Wi-Fi (5 GHz) or 2.4 GHz radio control. Tracked vehicle 'Onix' is operated by operator A, who is mainly in charge of work-related tasks. Mecanum rover and UAV are operated by operator B, who is in charge of visual inspection tasks.

Section 3.2 describes the design of the tracked vehicle Onix. This robot is designed to cover various tasks such as visual inspection, valve operation, and gas detection. It has accessibility to stairs and narrow passages so that it can cover all inspection passages except for cage ladders. The authors designed the robot to maximize the performance of mobility and dexterity. Especially, the design of a gripper is carefully considered in order to realize heavy-valve operation.

Section 3.3 describes the design of the mecanum-wheeled vehicle. This robot is used for visual inspection, especially in narrow passages. The authors selected an omni-directional rover as a platform because it has high positioning accuracy and smaller footprint than the tracked vehicle. Cameras are fixed at multiple heights because the height varies depending on the inspection target.

Section 3.4 describes the UAV design. This robot is used for visual inspection at high positions. The authors selected Mavic 2 Pro [14] as a platform considering its flight stability and space limitation of the environment. In order to apply the autonomous recognition to images from the UAV, we developed an image transportation system from the remote controller to the laptop computer.

Section 3.5 describes autonomous gauge reading from the camera images. The gauge is recognized in an image,

and its value is read by calculating the angle of the pointer. This module contributes to our high score of visual inspection in the competition, where we obtained 85% of the score of the visual inspection tasks in the final round.

3.2. Design of tracked vehicle

Onix consists of three major modules: tracks, arm, and gripper. The design of each module is described below.

3.2.1. Crawler design

Onix is a tracked vehicle consisting of two main crawlers covering the body and four subcrawlers (Figure 2), the design of which is based on FUHGA2 [15] and Quince [16]. The track of one main track and the two subtracks on the left and right sides are driven by the same motor. The crawlers are driven by a brushless motor, which is placed inside the drive pulley to reduce the size of the crawlers. Each of the four subcrawlers is driven by a servomotor through a pulley. The motor is selected to be able to climb a 45° slope.

One of the unique features of the Onix crawler design is that two of the four subcrawlers are connected to the main body with spacers in between to realize the transformation into small size while having a long subcrawler.

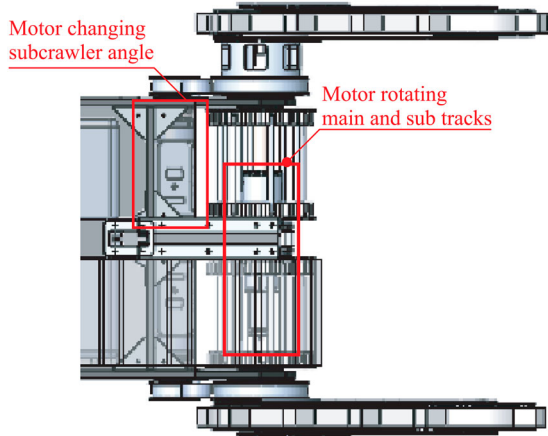


Figure 2. configuration of motor.

In the design of the tracked vehicle, the long subcrawlers bring various benefits. First, the performance of overcoming steps is improved, as shown in Figure 3. In addition, the robot can reach a higher position in the case of lifting the robot body by rotating the subcrawler downward, as shown in Figure 3(b), and working at a height with four legs. In contrast, as shown in Figure 4, if the vehicle has subcrawlers with a length larger than half of the main body, they collide with each other when rotating inward. Because they cannot be deformed sufficiently small, they contact with the movement of the vehicle in a confined space, limiting the vehicle's adaptive range. In Onix, two of the four subcrawlers are connected to the main body through spacers so that the front and rear subcrawlers do not contact with each other in their entire working range, as shown in Figure 5. To avoid conflict of subtracks, two configuration types such as diagonal configuration Figure 6(a) and parallel configuration Figure 6(b) can be considered. Basically, which subtracks are connected with the spacer can be selected at the time of assembly, and immediate configuration transformation is possible. Subsequently, we employed the diagonal configuration for the Onix design for the following reasons. Because Onix can view information about the environment through the front and rear cameras and both front and rear can be switched as the direction of travel, the subcrawlers seen by the camera should be equal in the front and rear directions. In the parallel configuration, the widths of the subcrawlers visible from the camera are different, which may cause confusion to the operator. Therefore, we employed the diagonal configuration, in which the positions of the robot and flipper coincide with those seen from the camera. Additionally, an operation is possible without a spacer. This configuration is advantageous because it minimizes the width when there are few obstacles in the upward direction.

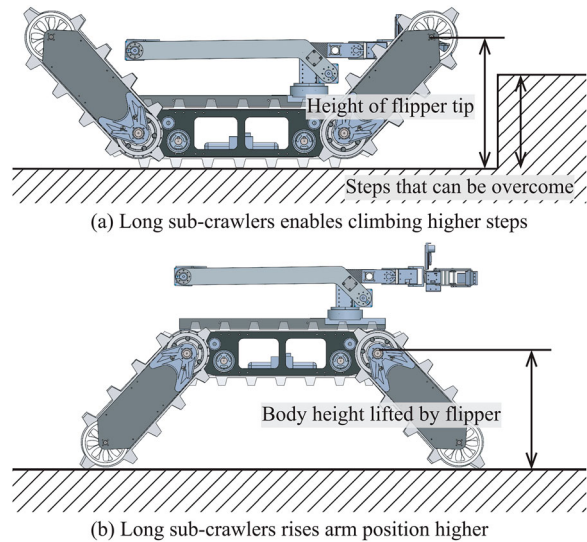


Figure 3. Benefit of the long flipper. (a) Long sub-crawlers enables climbing higher steps. (b) Long sub-crawlers rises arm position higher.

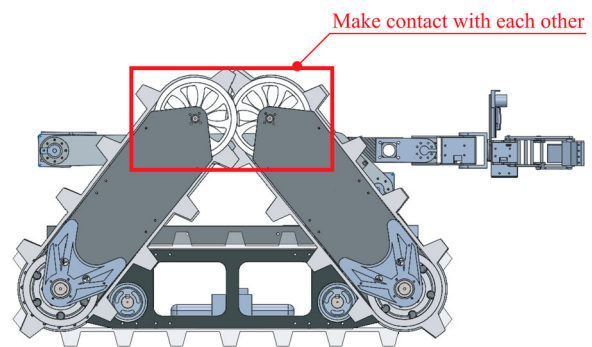


Figure 4. Conflict of subcrawler.

3.2.2. Arm design

The Onix arm has six DoF, and the motor is selected so that the payload of the paw is 3 kg. The length of each link is designed to fit into the robot body when viewed from above.

The arm of Onix is designed to support its own weight by the contact of each link when it is folded so that it remains stable even when the torque of the servomotor of each joint is lost. The arm position stability contributes to reducing the load on the motor when moving on uneven terrain, where large vibrations and inertial forces are generated. In addition, the components of each arm are designed to overlap when folded to reduce the folded size. To realize stable posture, an s-shaped sheet metal part is attached to the bottom of the upper arm as shown in Figure 7. Therefore, contacting points of the shoulder yaw motor and upper arm and forearm can support the weight of both arm links. Additionally, the gripper can be

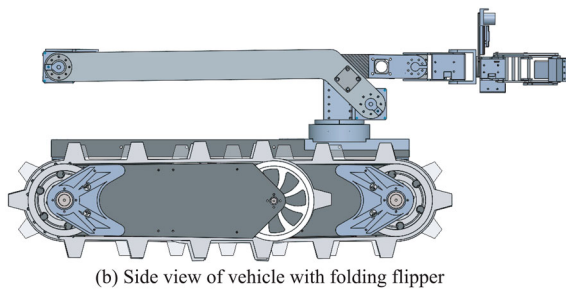
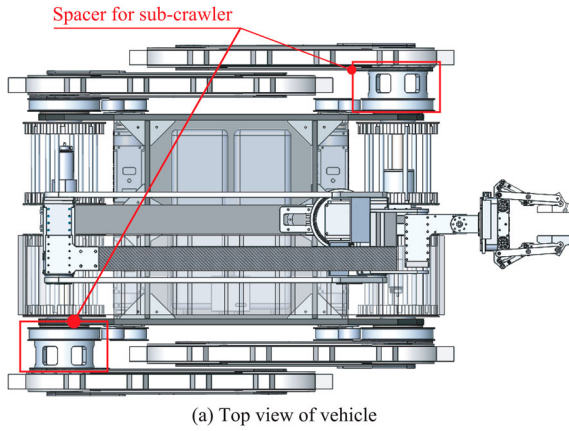


Figure 5. Folded flipper. (a) Top view of vehicle and (b) side view of vehicle with folding flipper.

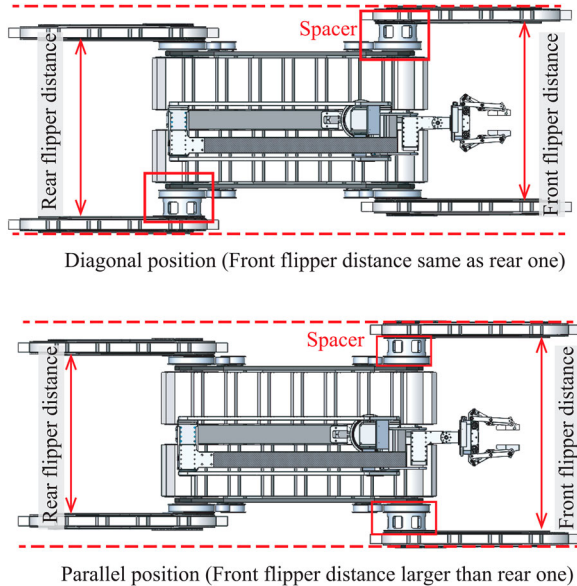


Figure 6. Difference of spacer configuration.

oriented and placed on the tip of the forearm to support its own weight (Figure 8).

3.2.3. Gripper

In Onix, two types of end-effectors are used as grippers depending on the situation so that the gripper can select the best end-effector for the purpose of plant inspection.

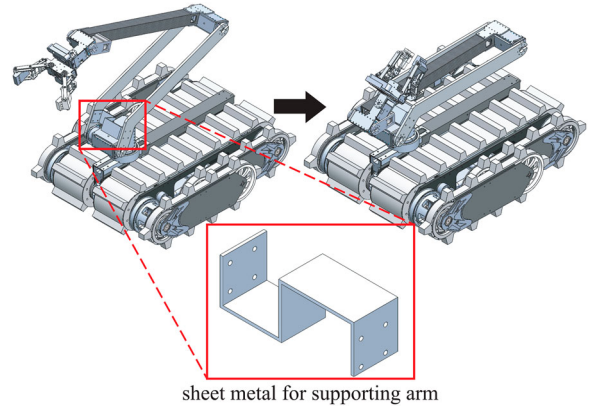


Figure 7. Vehicle with folded arm.

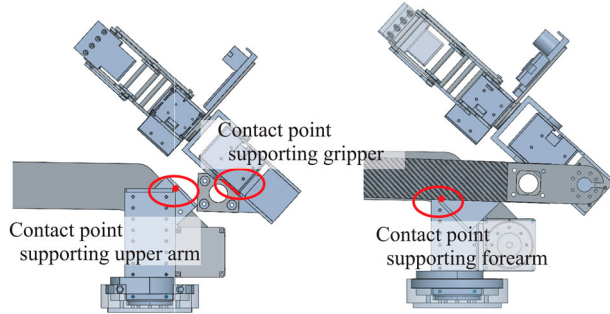


Figure 8. Contact point for supporting arm.

The first gripper is the Chebyshev hand [17], which has versatility and high gripping power. It is composed of superimposed Chebyshev links and parallel links as shown in Figure 10. The fingertips move along the linear trajectories of Chebyshev linkage (Figure 9); thus, the left and right fingers can be moved in the same straight line. In contrast, the gripper consists of only parallel links, which are installed in many robots, and the fingers move forward simultaneously when they are closed. Hence, the position of the finger shifts from the position of the object to be grasped, resulting in failure to grasp.

The Chebyshev hand is equipped with a rubber belt that covers not only the fingertips but also the inside of the hand to realize a large frictional holding force and a flexible grasping motion against the round and bar-shaped handles existing in the plant. First, for the round handle, as shown in Figure 11, the rubber belt touches a wide area on the side of the handle and can transmit a larger torque. Next, for the bar-shaped handle, because of the large holding force of the hand and the contact flexibility, the handle is not grasped with the fingertips but rather hooked on the inner space, as demonstrated in Figure 12. When the handle is grasped by fingertips and pulled with F_g in a direction that is off by an angle θ from the orthogonal direction to the handle as shown in

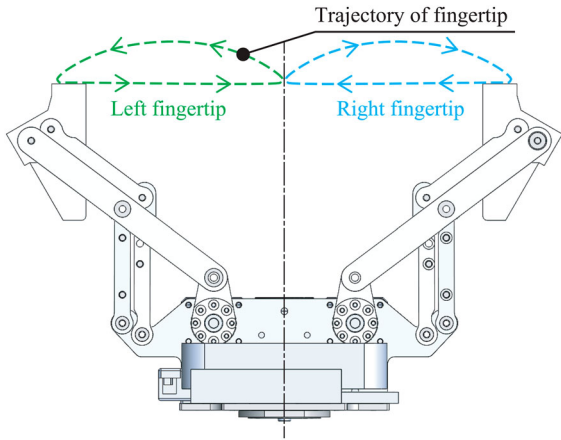


Figure 9. Chebyshev linkage hand has a straight trajectory, which aids human operation with high accuracy.

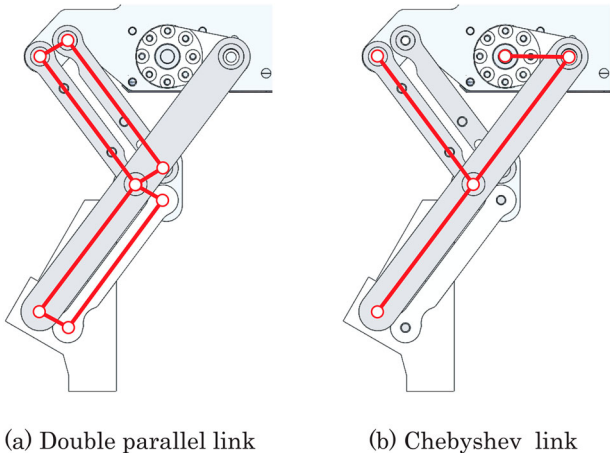


Figure 10. Configuration of linkage: our gripper consisted of double parallel linkage and Chebyshev lambda linkage.

Figure 13, The relationship between F_g , the force required to rotate the handle F_h , and frictional force F_g occurring in the direction perpendicular to F_h at the contact surface between the gripper and handle is expressed as follows:

$$F_h = F_g \cos \theta \quad (1)$$

$$F_f = F_g \sin \theta \quad (2)$$

If the object is grasped by the fingertips of the gripper, F_g must be less than the force that can be grasped by friction. From the above equation, as θ becomes larger, F_g also becomes larger, and thus slipping is more likely to occur. To manipulate a large bar handle, as shown in Figure 14, the handle should be pulled while changing the direction of the applied force as the handle rotates. When the center of rotation of the handle is known, the handle can be smoothly manipulated by calculating the exact trajectory. However, the position of the center is difficult to know in a plant with various handles. We solve this problem by adding flexibility to the contact on gripper. The gripper

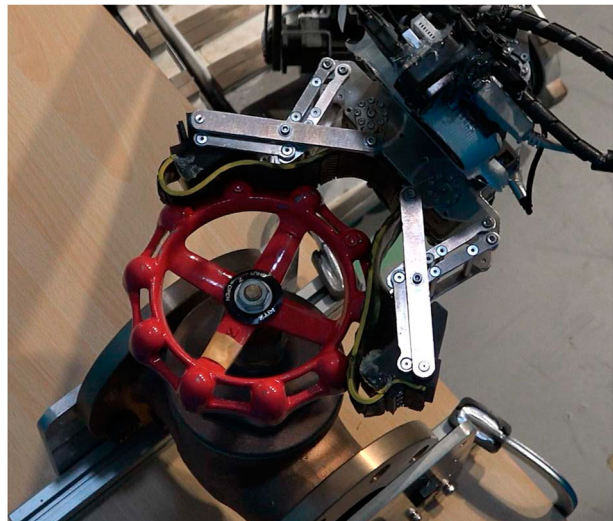


Figure 11. Grasp circular handle.

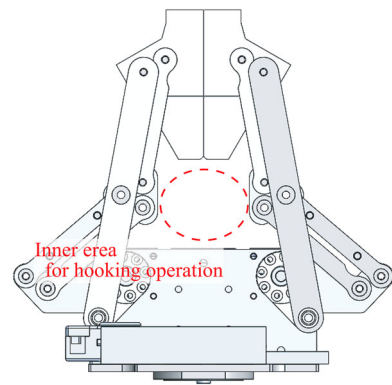


Figure 12. Ring-shaped area in Chebyshev-gripper.

can cause a contact force in the pulling direction and a frictional force in the longitudinal direction by hooking the handle in the ring-shaped space created when the fingers are closed (Figure 13). In addition, the clearance in the ring-shaped space permits misalignment of the angle between the handle and the gripper and allows operation without the need for precise positioning (Figure 15). In contrast, in the case of inner hooking, the friction coefficient of the contact area between the pipe and gripper are expressed as μ

$$F_g \sin \theta \leq \mu F_g \cos \theta \quad (3)$$

$$\theta \leq \arctan \mu \quad (4)$$

The second gripper is the belt-type end-effector that specializes in rotating handles, as shown in Figure 16. This end-effector can rotate a handle rapidly by circulating the belt after being hooked to the target circular handle as shown in Figure 17. In contrast to the Chebyshev

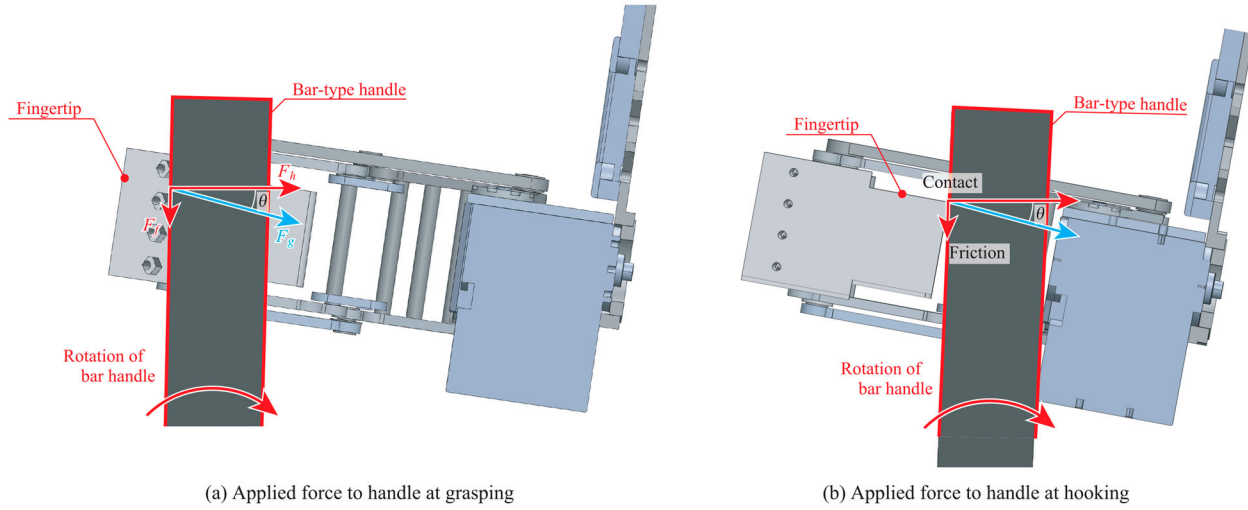


Figure 13. Relationship between bar handle and gripper.

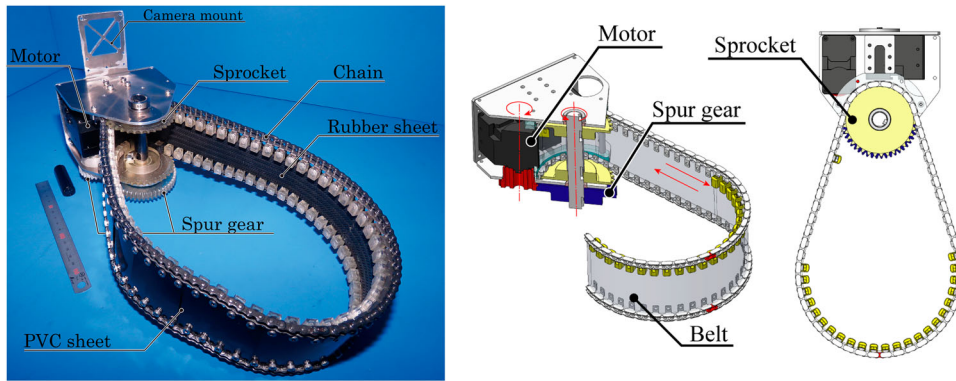


Figure 14. Grasp bar handle.

gripper, which can be used not only for manipulating the handle but also for grasping an object, the belt-type end-effector is less versatile but can perform the rotating motion of the handle at high speed. Therefore, considering the automation of plant inspection by robots, an end-effector specialized for this kind of rotating motion is necessary.

3.2.4. System configuration of Onix

Figure 18 shows the system configuration of Onix. The robot is operated from the operation station via Wi-Fi communication. In the robot, Intel's NUC computer with core-i7 processor is used for the control unit, in which Ubuntu 20.04 operating system is used and ROS noetic is used for middle ware. For tele-operation of chassis, fish-eye cameras are attached to the front and rear sides of the main body, and a spherical camera is attached to the elbow of the manipulator. Sensors for inspection: a visual camera, depth camera (realsense), thermal camera, and CO₂ sensor are attached to the end-effector. A 3D laser scanning sensor (Robosense RS-Bpearl) is attached

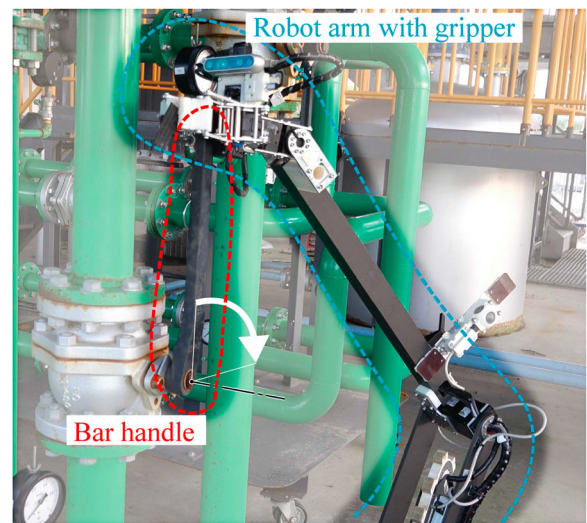
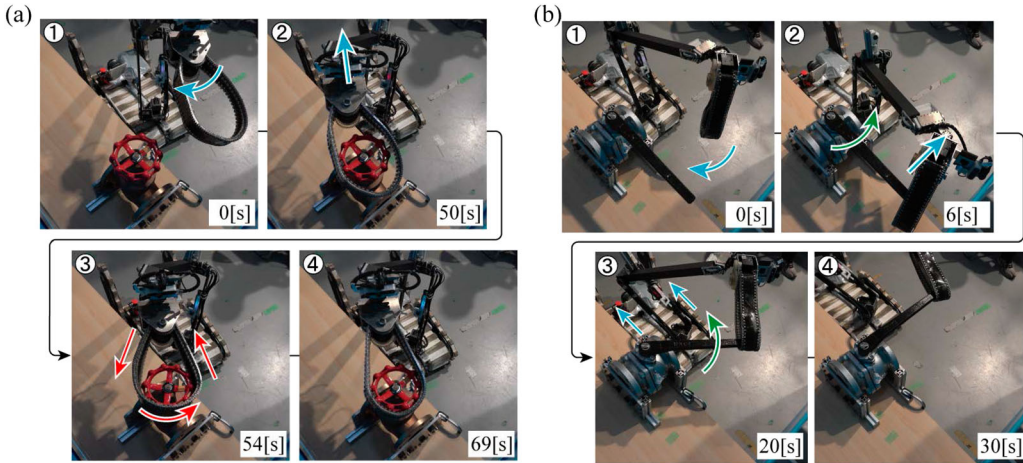
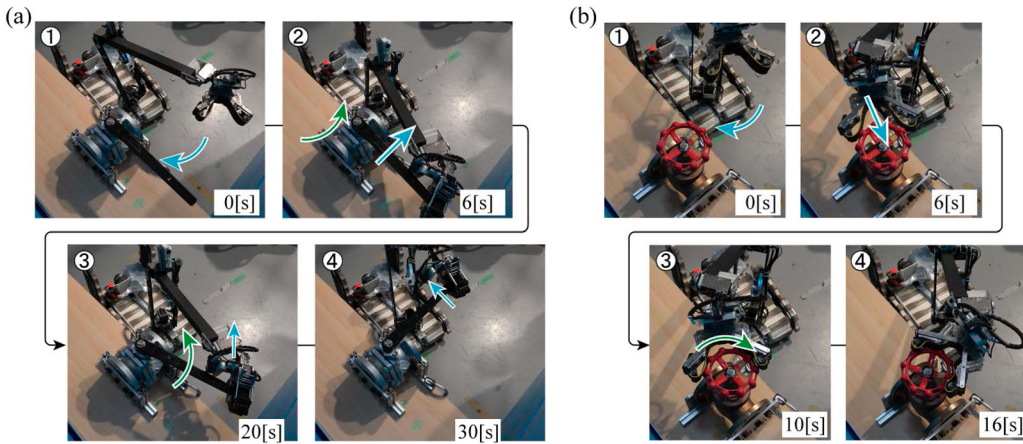


Figure 15. Rotate handle by Chebyshev gripper.

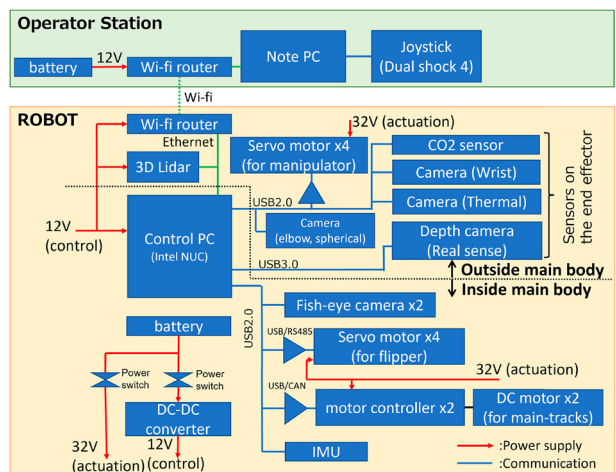
on the chassis for localization and mapping. Onix's chassis consists of two main tracks and four subtracks, which are actuated using brush-less DC motors and dynamixel's

**Figure 16.** Belt gripper.**Figure 17.** Rotate handle by belt gripper.

servomotors, respectively. The manipulator's joints and the gripper are actuated using dynamixel's servomotors. In the operator station, a note PC is used for observing the sensor data, including camera images and for sending motion commands to the robot. A Joystick is used for operating the chassis and the manipulator.

3.3. Design of mecanum-wheeled vehicle

To assign more specialized tasks to Onix, we developed a robot dedicated to the visual inspection task. Figure 19 shows mecanum-wheeled vehicle developed for visual inspection tasks. The purpose of this robot is a fast visual inspection in narrow passages with at least a 0.7 m width. For this, the robot has a four-wheeled mecanum that allows it to move freely even in narrow passages. It also has five cameras and two 3D lidars for high recognition capability. As this robot needed to be developed in a short time, we used many existing products. For the body, we used Viston's Mecanum Rover Ver. 2.1. For the frame to fix sensors, we used a general-purpose aluminum frame

**Figure 18.** System configuration of Onix. Red arrows show power supply, blue lines show USB connection, green lines show ethernet connection, and yellow lines show serial communication.

to reduce the machining time. We devised the sensor placement because this robot was primarily intended for visual inspection of pressure gauges. The position of



Figure 19. Mecanum-wheeled vehicle for visual inspection. This robot is mainly used for visual inspection in narrow passages. Cameras are fixed on multiple heights to inspect gauges installed at multiple heights.

the pressure gauge is generally fixed and can be known in advance. In particular, three different heights were employed in the WRS. Therefore, in this robot, the camera position was adjusted to accommodate all the heights. As a result, this robot could perform a visual inspection of a pressure gauge by simply moving in front of it.

3.4. Operational method of UAV

The authors selected DJI Mavic 2 pro [14] as a UAV platform, considering its flight stability, maximum running time, and space limitation in the inspection passages. DJI Mavic 2 pro has vision sensors in all directions for posture stabilization and collision avoidance. Because of the stability, this platform is used for exploration missions in other fields such as river water sampling missions [18]. Its maximum running time is 31 min at most, which exceeds the longest time of the mission in the WRS (30 min at the final). The body size is 497×431 mm; thus, it can



Figure 21. Gauge pointer extracted, and its rotation from 0 to 264 after binarization process.

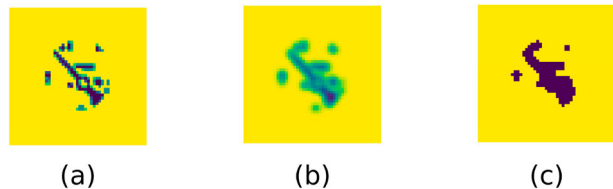


Figure 22. Gauge pointer extraction automatic process where: (a) dial ring is removed; (b) Gaussian blur is applied; (c) binarization and closing operations are applied.

rotate in the narrowest passage in the competition field (700 mm).

UAV's video stream is sent to a laptop computer, and used for image recognition as shown in Figure 1. A remote controller is connected to a smartphone, and the transmitted camera image from the drone is shown on the screen. The image is converted to HDMI using Google Chromecast. Subsequently, the image is converted again to USB using a HDMI-USB converter, which is connected to a computer via USB. The converter is determined as a USB camera by a computer so that the image is published as a ROS topic in the computer using a USB camera driver.

3.5. Gauge autonomous recognition

The gauge reading autonomous recognition used in this study can be divided into three steps: gauge location, pointer detection, and reading recognition. The image processing methods used in this work were performed using OpenCV [19]. The gauge location is represented by a square that indicates the gauge position in the image.

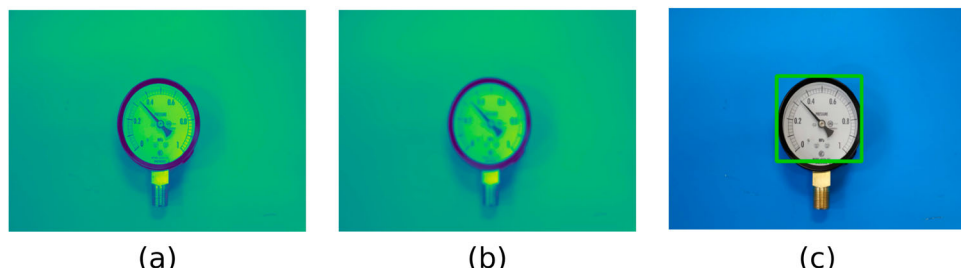


Figure 20. Gauge Location Extraction where: (a) shows the gauge L layer of LAB image; (b) shows the image after Gaussian blur; (c) shows the location of the image after Hough circle detection.

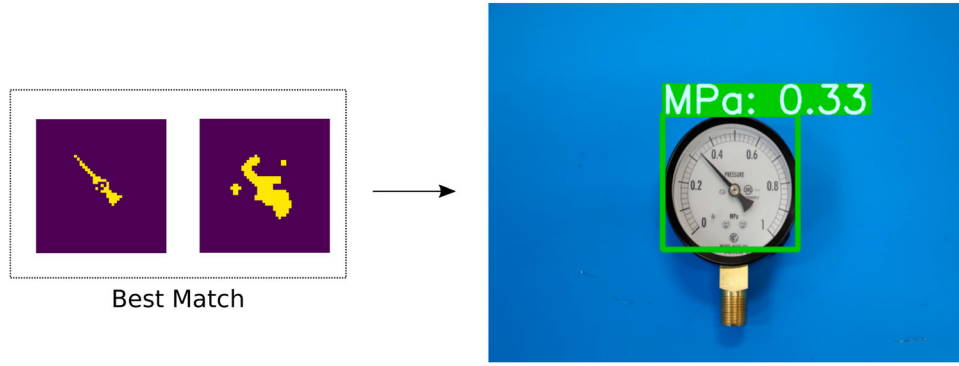


Figure 23. Final result showing the match pointer information and the actual MPa result from our approach.

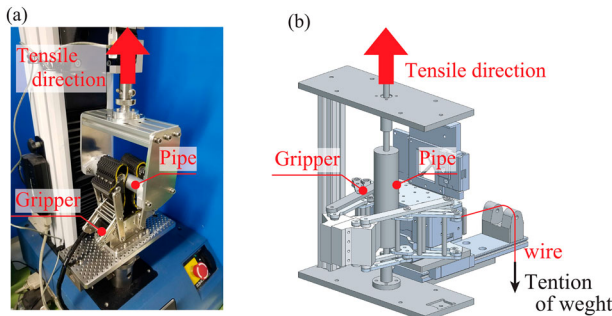


Figure 24. Rotate handle by belt.

In order to locate the gauge, the image is initially pre-processed to eliminate unnecessary information. In the preprocessing step, the image is converted from RGB to LAB, where the L layer of the image is extracted and then blurred using Gaussian blur. Subsequently, the Hough circle detection method can be used to determine the gauge position by searching for the gauge center in the preprocessed image information, as shown in Figure 20.

The pointer detection is performed by a template-based method. A pointer template is extracted manually beforehand, and after preprocessing the gauge image to clean the background area, the extracted pointer is used to determine the angle of the gauge pointer. Figure 21 shows the extracted pointer, which is used to rotate from 0 to 264° to match the template of the gauge pointer to be recognized.

The preprocessing step is performed to clean the gauge image in order to increase the accuracy of the template-based method in the following steps: first, the dial ring is segmented using the radius obtained from the Hough circle detection, as can be seen in Figure 22(a). Second, the image size is reduced, and blurring is performed using Gaussian blur to eliminate the gauge information written around the pointer, as can be seen in Figure 22(b). Third, binarization and closing operations are performed so that only the pointer can be seen in the image, as can be seen in Figure 22(c).

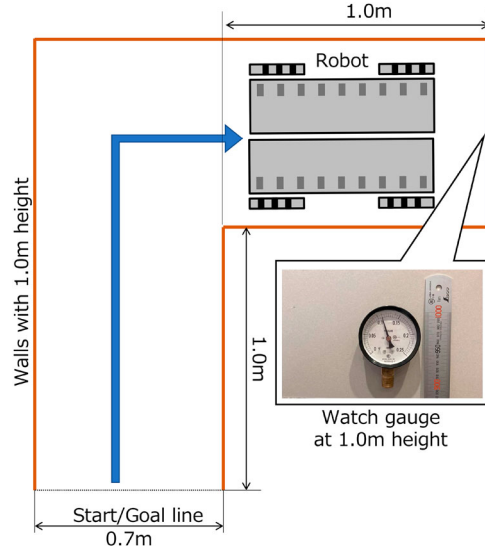


Figure 25. Setup of visual inspection in a narrow passage. The robot started from the start line, moved through the passage, read a gauge, and got back to the start position. Time is measured from when the robot enters the start/goal line to when it completely got out from the line.

Common template-based methods [20–22] are computationally expensive to search for the correct position of the pointer. Therefore, in this paper, we used a simplified version where the template is placed on the center of the gauge and rotated from the minimum dial ring to the maximum dial ring angle. For each iteration, we computed the similarity between the template and the actual gauge image, selecting the angle with the highest similarity. After obtaining the angle, the gauge pressure in megapascals can be computed as seen in Figure 23.

4. Evaluation

4.1. Holding performance of gripper with rubber belt

To evaluate the performance of the grasp bar handle, we measured two types of holding force by the



Figure 26. Setup of visual inspection on stairs. The robot started from the start line, climbed up stairs, read a gauge, and got back to the start position. Time is measured from when the robot enters the start/goal line to when it completely got out from the line.

the fingertips and by placing in the space inside the fingers (hold it like a gripper to hook it). The maximum force that the gripper can hold, while the pipe moves being pulled is measured as the holding force. The maximum tension applied to the pipe was set to 100 N to avoid destroying the mechanism. The directions of the gripper and pipe were measured in two directions: the direction when the handle was pulled. In the experiment in (a), the motor that moved the fingers rotated with a constant torque, and the measurement was performed at five different levels of torque. In the experiment (b), the direction of the gripper was changed by 90°, and the holding force was measured when the pipe was pulled in the orthogonal direction. In this experiment, after gripping the pipe with the gripper, a force was applied to the pipe in the direction of pulling with a wire to which a weight is attached, and then the measurement was performed. In the case of grasping with the fingertips, the mass of the weight was set at five levels from 0.5 to 2.5 kg, which is the weight that can be held by fingertip grasping based on the experimental results in (a). In the case of hooking with the inside of the finger, the weights ranged from 1 to 5 kg.

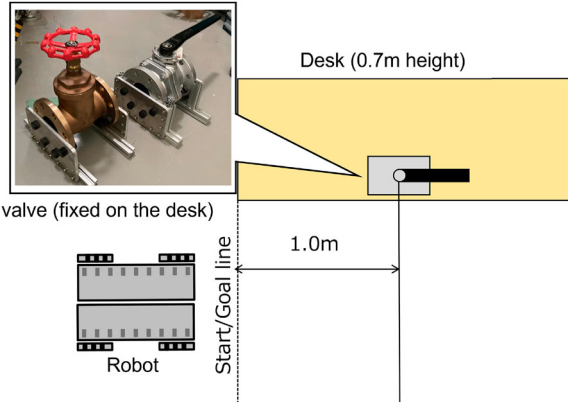


Figure 27. Setup of valve operation. The robot started from the start line, operated the valve, and returned to the start position. This test was conducted on the circular valve and lever valve, respectively. The time was measured from when the robot entered the start/goal line to when it completely exited from the line.

Chebyshev gripper with a covering rubber belt. As shown in Figure 24, the force generated when operating the handle is divided into two forces: (a) in the direction of pulling the bar handle and (b) in the centrifugal direction, orthogonal to (a). In both experiments, a Chebyshev gripper and a metal pipe of 25 mm diameter were mounted on a tensile testing machine, and the holding force was measured by pulling the gripped pipe. In addition, the pipe could be grasped in two ways: with

4.2. Performance comparison of different type of robots

To clarify the individual performance and difference between the robots, three types of the experiment was conducted as follows:

- (1) visual inspection in a narrow passage with an L-shaped curve (Onix, mecanum, UAV);
- (2) visual inspection in a passage with stairs (Onix, UAV);
- (3) large valve operation (Onix).

In all experiments, time was measured during the robot performing the single task, and the same trial was conducted for 10 times. (1) Was conducted to see the performance in the narrow space, because inspection passage tends to be narrow due to limited facility placement. (2) Was conducted on Onix and UAV to test the accessibility to high positions. (3) Was conducted on a circular valve and lever valve to evaluate Onix's performance of large valve operation. The details of each test are shown below.

4.2.1. Visual inspection in a narrow passage with L-shaped curve

Figure 25 shows the setup of visual inspection in the narrow passage with an L-shaped curve. The robot started from the start line, moved through the passage, read a

gauge, and returned to the start position. The time was measured from when the robot entered the start/goal line to when it completely exited the line. The passage width (0.7 m) was decided based on the minimum width of the passage in the competition field that we measured during pre-practice. This test was conducted on Onix, mecanum rover, and UAV. In the case of UAV, movement over the wall was prohibited considering the real situation where the passage is attached between the facilities and there is no space between the sealing and the facility.

4.2.2. Visual inspection on stairs

Figure 26 shows the setup of visual inspection in the narrow space. The robot started from the start line, climbed up stairs, read a gauge, and returned to the start position. The time was measured as same way as above. This test was conducted on Onix and UAV.

4.2.3. Large valve operation

Figure 27 shows the setup of valve operation. The robot started from the start line, operated the valve, and returned to the start position. This test was conducted on the circular valve and lever valve, respectively. The valve was rotated by 180° in the case of the circular valve and 90° in the case of lever valve. The valve type was selected based on the rule book of the competition [13], where ‘KITZ Corporation Class 150 Cast Bronze Gate Valve, EBH (80A)’ was used as circular valve and ‘KITZ Corporation 10 K Cast Iron Ball Valve, 10FCTB (50A, 80A)’ as lever valve. This test was conducted on Onix.

4.3. Total performance based on scores in the competition

The total performance of the proposed system was tested in the competition, and the results were analyzed based on the scores. Here, the results of the final round are analyzed because the daily inspection scenario (visual inspection, valve operation) and emergency response (debris removing, finding victims) are included as described in Section 1. The overview of the tasks is described in [2]. The time for the mission was 30 min, in which daily inspection tasks were conducted in the former 15 min and emergency response tasks in the latter 15 min.

In the competition, we used onix with the following configuration. The crawler is set without spacers to reduce the width of the robot because the field of competition does not have low ceilings but narrow passageways. We used only the Chebyshev gripper instead of the belt gripper, which was adapted to operation for bar and circular handle. But the handles in the competition field are in confined spaces where the belt gripper was difficult to insert. The miniaturization of the belt gripper suitable for the field is the next challenge for this project.

The results are based on self-scoring using the report we submitted after the mission, gathered data during the mission, and total score announced by organizers (440). To clarify the contribution of each robot, the breakdown of score by robots was calculated. The score rate of each task to the full score was also calculated to clarify the room of obtaining more scores.

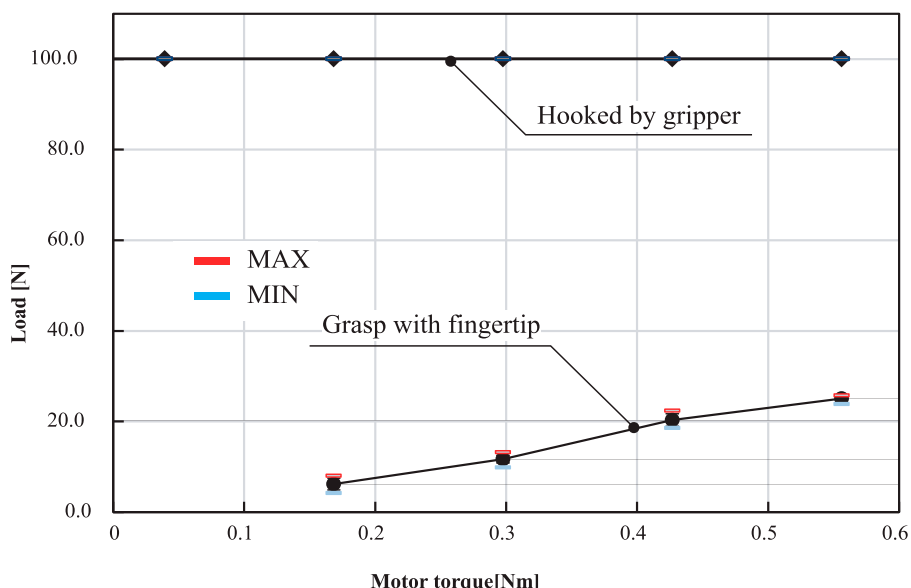


Figure 28. Result of holding performance: comparison for range of handling load capacity with grasping and hooking by Chebyshev’s hand.

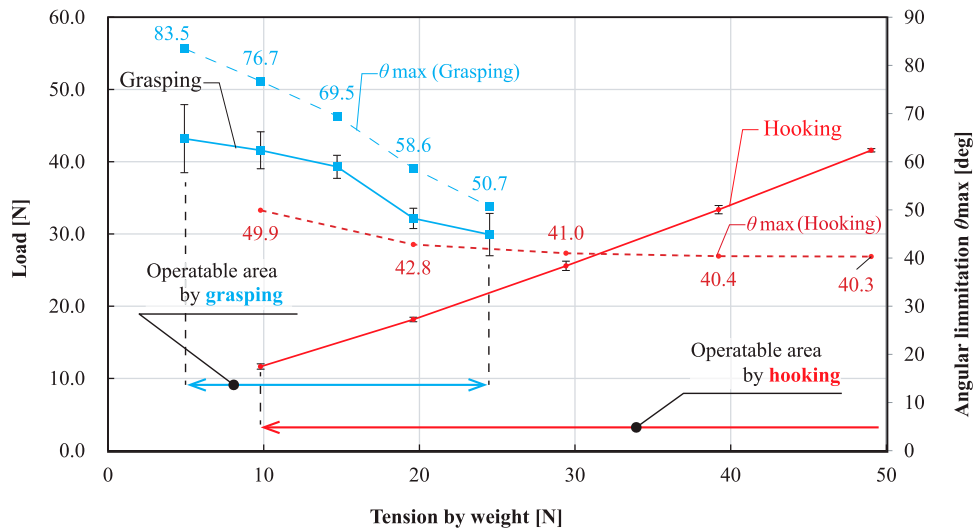


Figure 29. Holding force measurement results in an orthogonal direction.

5. Results

5.1. Holding performance of gripper with rubber belt

Figure 28 shows the holding force results. In the graphs, the dotted line and the practice show the average value of the holding force of the pipe when the pipe was held between the fingertips and when the pipe was scratched inward, respectively. The red and blue bars show the maximum and minimum values, respectively. In the case of hooking the pipe on the inside, the pipe did not come off even when a load of 100 N was applied. Contrarily, when grasping with the fingertips, the maximum holding force was about 25 N. Next, the grasping force in the orthogonal direction is shown in Figure 29. In the graph, as in Figure 28, the dotted line and the practice show the holding force of the pipe when the pipe is grasped with the fingertips and when the pipe is scratched inward, respectively. Additionally, the red line shows the allowable error angle when the weight tension is applied to Equation (2). From the graphs, it was found that the orthogonal holding force decreased in the fingertip grasping and increased in the inner hooking when the tensile force by the weight was increased.

5.2. Performance comparison of different type of robots

Table 2 shows the results of individual performance tests of the robots. In the visual inspection in a narrow passage, Onix took 89.7 s, mecanum rover took 37.6 s, and UAV took 61.5 s, on average. These results show that the mecanum rover was the fastest, 58% faster than that of Onix. In the visual inspection on stairs, Onix took 107.9 s

Table 2. Performance of the individual robots.

Task	Robot	Time (s) ($n = 10$)
Narrow passage	Onix	89.7 ± 8.9
	Mecanum	37.6 ± 5.6
Stair climbing	Onix	61.5 ± 13.9
	UAV	107.9 ± 11.2
Valve (circular)	Onix	55.6 ± 9.4
	Onix	100.8 ± 32.2
Valve (lever)	Onix	65.5 ± 14.2

Time is described as mean \pm SD (s).

and UAV took 55.6 s, on average. These results show that the UAV was 48% faster than that of Onix. In the valve operation by Onix, circular valve operation took 100.8 s, and lever valve operation took 65.5 s on average.

5.3. Total performance based on scores in the competition

Table 3 shows the raw scores of the mission. In the table, the score is for each robot in the row and for each task in the column.

Figure 30 shows the breakdown of the total scores by robots. The percentage of scores of Onix, mecanum, and UAV were 48%, 36%, and 16%, respectively. Onix was operated by operator A, and mecanum vehicle and UAV by operator B. This result shows that the two operators equally contributed to the total score.

Figure 31 shows the score rate of each task to the full score. The rate was 85% in visual inspection, 57% in valve operation, and 92% in emergency response. It shows the high score rate in visual inspection and emergency response, and room for obtaining more score in valve operation.

Table 3. Received points in the final round of the competition.

Robots	Daily inspection tasks		Emergency response tasks			Total for each robot
	Visual inspection	Valve operation	Route traversing	Debris removing	Searching victims	
Onix	0	160	10	40	0	210
Mecanum	130	0	20	0	10	160
UAV	40	0	20	0	10	70
Total for each task (Full score)	170 (200)	160 (280)	50 (50)	40 (50)	20 (20)	440 (600)

This table is based on self-scoring using inspection report that we wrote during the competition, and total score announced by the organizer.

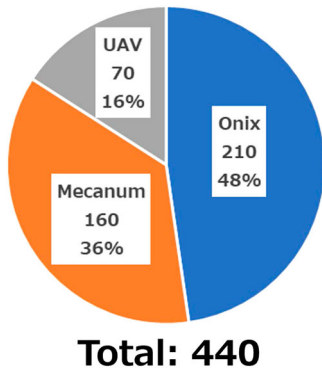


Figure 30. Breakdown of total scores by robots. Onix was operated by operator A, and Mecanum vehicle and UAV were operated by operator B. This result shows that the two operators equally contributed to the total score.

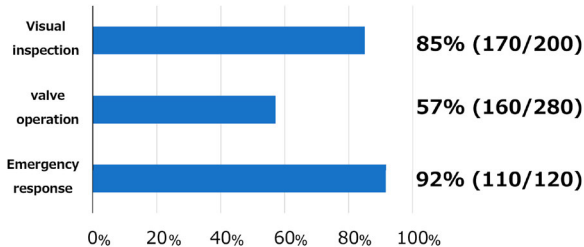


Figure 31. Score rate of each task to the full score. The rate was 85% in visual inspection, 57% in valve operation, and 92% in emergency response. It shows the high score rate in visual inspection and emergency response, and room for obtaining more score in valve operation.

6. Discussion

From the measurement experiment of the holding force of the gripper, the range of good performance was found for both fingertip grasping and inner hooking. First of all, the maximum holding force in the tensile direction for the fingertip grasp in Figure 28 was 25 N, while the inner hooking was able to hold the tension of over 100 N. In addition, the inner hooking has the same retention performance even at low torque, which means that the inner hooking can be operated with lower power consumption than the fingertip grasping. In addition, as shown in Figure 29, the frictional holding force in the orthogonal direction with hooking pipe, which is necessary for the

operation of the bar handle, also increased as the tension increases. Based on the experimental results, the allowable angle difference was calculated to be more than 40°, which indicates that the geometric angle limit of the gripper is sufficiently acceptable. However, the orthogonal holding force when the tensile force was smaller than that of the fingertip grasp. On the other hand, in the fingertip grasp, the orthogonal holding force became smaller as the load became larger. This is because it is determined by the combined force of the weight and the tension as shown in Section 3.2.3. This is because it is determined by the combined force of the generated forces. However, if the load is within 25 N, which is the maximum load that can be grasped under the conditions of this paper, the limitation angle is more than 50°, so it is possible to use the handle even if it cannot pull it vertically. Therefore, fingertip grasping with high holding force in all directions is effective for applying small force such as grasping a light object, and it is effective for pulling a heavy object or operating a hard bar handle. Especially, the high holding force is effective for opening and closing the valve under pressure and working on the rusty handle in the Outdoors.

The results of the individual performance test of robots show that the visual inspection task is completed 58% faster when the mecanum vehicle is used in the narrow passage and 48% faster when the UAV is used on the stairs, as compared with the tracked vehicle in the same situation. These results show the advantage of our strategy in increasing the time efficiency of the visual inspection tasks using the mecanum wheeled vehicle in narrow passages and the UAV at high positions. This is one solution to conduct the tasks efficiently using different types of robots, as suggested in [1].

According to the total performance in the competition described in Section 5.3, our system obtained 85% points in the visual inspection tasks and 57% points in the work-related tasks. We obtained the highest score among the teams advancing to the finals. In the final round, the visual inspection in the former part (daily inspection) was completed within 5 min, which was considerably faster than that of the time limitation (15 min) so that one operator did nothing for the rest 10 min. This

is a result of our strategy to increase the time efficiency of visual inspection using a heterogeneous robot system. During the mission, mecanum vehicle was used for visual inspection in a narrow passage, UAV was used for visual inspection in high position, and onix concentrated on valve operation considering the results in individual performance in Table 2. The high time efficiency in the visual inspection tasks cannot be achieved by homogeneous configuration where visual inspection is conducted by another Onix, because time for visual inspection should be more than doubled considering the individual performance in a narrow passage and stair climbing shown in Table 2. Meanwhile, this freed-up time can be used for work-related tasks that cannot be performed within the time limit. The authors suggest two ways of further performance improvement:

- Introducing additional robot just for work-related tasks.
- Attaching end-effector on mecanum vehicle to operate small valves.

In both cases, the rest time of the visual inspection can be used for work-related tasks.

The authors also found some rooms for improvement in the current direction. For example, gauge reading would be easier if cameras on the mecanum rover have pan-tilt active gimbal, whereas the camera's direction is adjusted only by the chassis in the current system. The UAV's flight would be safer if additional cameras are attached in upward and downward, especially when it flies in narrow and complicated environment.

The authors assume that the two operators with proposed robot configuration were the best in the situation where the robots need to share the same passage during the tasks at the field with 130 m² area in the competition. During the competition, operators tried to share the same inspection passage by multiple robots and conducted tasks in different positions. Although more robots could be operated simultaneously if an operator is added, it might cause conflict of robot traffic in the limited space. To scale our proposed system for larger area in the real situation, it is desirable to have multiple system sets in different locations to avoid the conflict and to keep high time efficiency. Or, higher-level traffic control would be helpful for increasing density of the robot in a limited space.

Throughout the competition, the authors found that the environmental factors make the tasks more difficult. West sun lowers recognition success rate, or the large valves become heavier due to rusting, for instance. Such findings should be reflected to the latter development, not

only for mechanical design but also for software design such as autonomous recognition.

7. Conclusion

In this study, the authors developed a plant inspection system using three different types of robots responsible for winning the WRS 2020 plant disaster prevention challenge. The design of each robot is described showing the features of the robots and the recognition systems used in the competition. The use of a multi-robot system enhances the overall performance because of task specialization. The results show that according to the scenario that favors the type of robot, the visual inspection task performance can be increased to 58% and 48% by using a mecanum vehicle and a UAV, respectively, as compared with the tracked vehicle in the same situations. Moreover, the analysis of the tracked vehicle novel grip design shows an increase in the performance in the case of large-structure manipulation owing to the extension of the contact area, which allows for higher friction. Finally, based on the total performance in the competition, our system obtained 85% points in the visual inspection tasks, 57% points in the work-related tasks, and 92% of the emergency response tasks.

Disclosure statement

No potential conflict of interest was reported by the author(s).

Funding

Robot development in this study was supported by the WRS 2020 Team Support Program.

Notes on contributors

Shotaro Kojima is currently an assistant professor at New Industry Creation Hatchery Center of Tohoku University, Japan. He is also a project assistant professor at the Tough Cyberphysical AI Research Center of Tohoku University. He received his Ph.D. degree and M.Sc. in Information Sciences from Tohoku University in 2021 and 2017, respectively. He received his B.Sc. in Mechanical engineering from Tohoku University in 2015. His research interests are robot navigation systems and disaster responding robots. A member of RSJ, JSME and IEEE.

Tomoya Takahashi is currently a Ph.D. student at the Graduate School of Information Science of Tohoku University, Japan. His research involves a bioinspired mechanism composed of soft materials and a robotic mechanism for disaster sites. He received his M.Sc. in Information Science from Tohoku University in 2021. He received his B.Sc. in Engineering from the National Institute of Technology, Nagaoka College, Japan in 2019. A member of RSJ, SICE, and IEEE.

Ranulfo Bezerra is currently a researcher at the Tough Cyberphysical AI Research Center of Tohoku University. His research involves autonomous vehicle recognition systems and multi-agent task allocation and navigation systems. He received his Ph.D. degree in Information Sciences from Tohoku University, Japan, in 2021. He received his M.Sc. and B.Sc. in computer science from the Federal University of Piaui, Brazil, in 2018 and 2016, respectively. His research interests are robot intelligence, robotic perception, and multi-robot systems. A member of RSJ and IEEE.

Takaaki Nara is currently a Master's student at the Graduate School of Information Sciences, Tohoku University, Japan. He received his B.Sc. in Electrical engineering from the Tokyo University of Agriculture and Technology, Japan, in 2021. His research interests are swarm robot localization and disaster responding robots. A member of RSJ and IEEE.

Masaki Takahashi had belonged to the Graduate School of Information Sciences, Tohoku University, Japan until March 2022. He received his M.Sc. in Information Sciences from Tohoku University in 2022. He received his B.Sc. in Mechanical engineering from Tohoku University in 2019. His research interests is drone with center of gravity adjustment. A member of RSJ and JSME.

Naoto Saiki had belonged to the Graduate School of Information Sciences, Tohoku University, Japan until March 2022. He received his M.Sc. in Information Sciences from Tohoku University in 2022. He received his B.Sc. in Mechanical Engineering from Tohoku University in 2019. His research interests are spherical parallel mechanisms and omnidirectional mechanisms. A member of RSJ and JSME.

Kenta Gunji is currently a Ph.D. student at the Graduate School of Information Science of Tohoku University, Japan. He also served as media co-chair at the Student Activities Committee of the IEEE Robotics and Automation Society. His research involves SLAM techniques that enable stable autonomous mobility in environments where the arrangement of objects can change. He received his M.Sc. in Information Science from Tohoku University in 2022. He received his B.Sc. in Engineering from the Faculty of Science and Technology, Keio University, Japan in 2020. A member of JSME and IEEE.

Pongsakorn Songsuroj had belonged to the Graduate School of Information Sciences, Tohoku University, Japan until March 2022. He received his M.Sc. in Information Sciences from Tohoku University in 2022. He received his B.E. in Electrical Engineering from King Mongkut's Institute of Technology Ladkrabang in 2014. His research interests are aerial robotics and control system. A member of JSME.

Ryota Suzuki had belonged to the Graduate School of Information Sciences, Tohoku University, Japan until March 2022. He received his M.Sc. in Information Sciences from Tohoku University in 2022. He received his B.Sc. in Sciences and Engineering from Fukushima University in 2020. His research interests are multi-robot system and optimal control. A member of JSME.

Kotaro Sato had belonged to the Graduate School of Information Sciences, Tohoku University, Japan until March 2022. He received his M.Sc. in Information Sciences from Tohoku

University in 2022. He received his B.Sc. in Sciences and Engineering from Fukushima University in 2020. His research interests are cyber-enhanced canine. A member of JSME.

Zitong Han is currently a Ph.D. student at the Graduate School of Information Science of Tohoku University, Japan. His research involves tethered UAV systems. He received his M.Sc. in Information Science from Tohoku University in 2021. He received his B.Sc. in Engineering from Shibaura Institute of Technology, Japan in 2019. A member of RSJ and IEEE.

Kagetora Takahashi is currently a master's student at Tohoku University, Japan. He received his B.Sc. in Mechanical Engineering from Kanazawa University in 2021. His research interests are robot mechanism and variable stiffness mechanism. A member of RSJ and IEEE.

Yoshito Okada received his Ph.D. in Engineering from Tohoku University, Japan in 2012. He was a visiting researcher at Field Robotics Center of Carnegie Mellon University, USA in 2013 and an assistant professor of Tohoku University in 2014. He was a research scientist at the RIKEN Center for AIP. He is now a project associate professor at the Tough Cyberphysical AI Research Center of Tohoku University. A member of RSJ, SICE, JSME and IEEE.

Masahiro Watanabe is currently an Assistant Professor at Tough Cyberphysical AI Research Center of Tohoku University. He received B.S., M.S., and Ph.D. degrees in Engineering all from Tokyo Institute of Technology, Tokyo, Japan, in 2013, 2015, and 2018, respectively. His research interests are soft robotics and disaster responding robots. He is a member of RSJ, JSME, and IEEE.

Kenjiro Tadakuma holds an Associate Professorship at Tohoku University in the field of robotics, where he has been leading the Plus Ultra Mechanism Group since 2015. Throughout his career, he has made outstanding contributions to the design of novel robotic mechanisms. As a Ph.D. student at Tokyo Tech (2004–2007), he invented the first omnidirectional mechanism, known as 'Omni-Ball'. This brought him to MIT's Field and Space Robotics laboratory as a post-doctoral researcher (2007), where he went on to contribute to the Mars hopper project and developed a polymer-based mechanical device for medical applications. Back in Japan, he held positions at Tohoku University, the University of Electro-Communications, and Osaka University (2008–2015), where he expanded on the concept of omnidirectional mechanisms with successful applications in mobile robotics and gripping mechanisms, such as the 'Omni-Crawler' and 'Omni-Gripper'. At Tohoku University, he is further trying to extract the essence of biological mechanisms to express them as robotic mechanisms. The nature of his inventions illustrates his deep focus in pioneering the field of robotics mechanisms as fundamental science. A member of RSJ, JSME and IEEE.

Kazunori Ohno received B.S., M.S., and Ph.D. in Engineering from Tsukuba University in 1999, 2001, and 2004. He was a COE researcher at Kobe University in 2004, became an assistant professor, a lecturer, and an associated professor at Tohoku University in 2005, 2008, and 2012, and has been a specially appointed professor at New Industry Creation Hatchery Center (NICHe) Tohoku University since 2021. He was also a PRESTO researcher (2008–2012) and has been a visiting researcher of the

RIKEN Center of AIP (2017–2021). His research fields are field robotics, robot intelligence, and cyber-enhanced canines. He established TC on Data Engineering Robotics of RSJ in 2012. He received Kiso awards in 2008 and 2012, and RSJ research awards in 2005 and 2019. A member of RSJ, JSME, VRSJ, JSAE, IEEE.

Satoshi Tadokoro graduated from the University of Tokyo in 1984. He was an associate professor at Kobe University from 1993 to 2005, and has been a Professor of Tohoku University since 2005. He was a Vice/Deputy Dean of Graduate School of Information Sciences from 2012 to 2014, and has been the Director of Tough Cyberphysical AI Research Center since 2019 at Tohoku University. He has been the President of the International Rescue System Institute since 2002, and was the President of IEEE Robotics and Automation Society in 2016–2017. He served as the Program Manager of MEXT DDT Project on rescue robotics in 2002–2007, and was the Project Manager of Japan Cabinet Office ImPACT Tough Robotics Challenge Project on disaster robotics in 2014–2019 having 62 international PIs and 300 researchers that created Cyber Rescue Canine, Dragon Firefighter, etc. His research team in Tohoku University has developed various rescue robots, two of which are called Quince and Active Scope Camera are widely recognized for their contribution to disaster response, including missions in the Fukushima-Daiichi NPP nuclear reactor buildings. IEEE Fellow, RSJ Fellow, JSME Fellow, and SICE Fellow.

ORCID

Kenjiro Tadakuma  <http://orcid.org/0000-0003-2035-0617>
Kazunori Ohno  <http://orcid.org/0000-0003-3958-2901>

References

- [1] Sprint robotics roadmap February 2018. SPRINT Robotics. 2018.
- [2] Tadokoro S, Kimura T, Okugawa M, et al. The world robot summit disaster robotics category—achievements of the 2018 preliminary competition. *Adv Robot*. 2019;33(17):854–875.
- [3] Iagnemma K, Buehler M. Editorial for journal of field robotics: special issue on the DARPA grand challenge. *J Field Robot*. 2006;23(9):655–656.
- [4] Buehler M, Iagnemma K, Singh S. The DARPA urban challenge: autonomous vehicles in city traffic. Vol. 156. New York (NY): Springer; 2009.
- [5] International aerial robotics competition [cited 2022 Feb 17]. Available from: <http://www.aerialroboticscompetition.org>
- [6] Robocup. [cited 2022 Feb 17]. Available from: <http://www.robocup.org>
- [7] Shukutani K, Onishi K, Onishi N, et al. Development of explosion-proof autonomous plant operation robot for petrochemical plants. *Mitsubishi Heavy Ind Tech Rev*. 2018;55(4):1–6.
- [8] Fujita J, Souda D, Murata C, et al. The development of robots for the nuclear power plants and their application to new fields. *Mitsubishi Heavy Ind Tech Rev*. 2020;57(4):1–6.
- [9] Biegl M, Hasenauer R, Silberbauer L, et al. Marketing testbeds for high tech innovation: The case of taurob robotics. *Proceedings of picmet '14 conference: Portland international center for management of engineering and technology; infrastructure and service integration*. Kanazawa: IEEE. 2014. p. 1145–1168.
- [10] Miura H, Watanabe A, Okugawa M, et al. Plant inspection by using a ground vehicle and an aerial robot: lessons learned from plant disaster prevention challenge in world robot summit 2018. *Adv Robot*. 2020;34(2):104–118.
- [11] Tanaka M, Kon K, Nakajima M, et al. Development and field test of the articulated mobile robot T² Snake-4 for plant disaster prevention. *Adv Robot*. 2020;34(2):70–88.
- [12] Matsumoto N, Tanaka M, Nakajima M, et al. Development of a folding arm on an articulated mobile robot for plant disaster prevention. *Adv Robot*. 2020;34(2):89–103.
- [13] World robot summit 2020 disaster robotics category: plant disaster prevention challenge competition rules ver. 1.53. [cited 2022 Feb 17]. Available from: https://wrs.nedo.go.jp/wrs2020/challenge/download/Rules/DetailedRules_Plant_EN.pdf
- [14] Dji mavic 2. [cited 2022 Feb 17]. Available from: <https://www.dji.com/en/mavic-2>
- [15] Takemori T, Miyake M, Hirai T, et al. Development of the multifunctional rescue robot fuhga2 and evaluation at the world robot summit 2018. *Adv Robot*. 2020;34(2):119–131.
- [16] Rohmer E, Ohno K, Yoshida T, et al. Integration of a sub-crawlers' autonomous control in quince highly mobile rescue robot. In: 2010 IEEE/SICE International Symposium on System Integration. Sendai: IEEE. 2010. p. 78–83.
- [17] Takahashi T, Okada Y, Kojima S, et al. Design and control of parallel gripper with linear and curved trajectory consisting of only revolute pairs. *2020 IEEE/SICE International Symposium on System Integration (SII)*. Honolulu: IEEE. 2020. p. 557–562.
- [18] Vellemu EC, Katonda V, Yawuwa H, et al. Using the Mavic 2 Pro drone for basic water quality assessment. *Scientific African*. 2021;14:e00979.
- [19] Bradski G. The OpenCV library. *Dr Dobb's Journal of Software Tools*. 2000.
- [20] Pirzadeh H. Computational geometry with the rotating calipers. Montreal: McGill University. 1999.
- [21] Baig AQ, Naeem M, Gao W. Revan and hyper-Revan indices of octahedral and icosahedral networks. *Appl Math Nonlinear Sci*. 2018;3(1):33–40.
- [22] Gao W, Wang W. A tight neighborhood union condition on fractional (g, f, n', m) -critical deleted graphs. In: *Colloquium mathematicum*. Vol. 149. Warsaw: Instytut Matematyczny Polskiej Akademii Nauk; 2017. p. 291–298.